論文 / 著書情報
Article / Book Information

論題(和文)	
Title(English)	Zero-Crossing-Rate Based Global Damping Model of VE Systems Considering Frequency Sensitivity
著者(和文)	張庭維, 佐藤大樹
Authors(English)	Ting-Wei Chang, Daiki Sato
出典(和文)	日本建築学会大会学術講演梗概集, 構造II, , pp. 511-512
Citation(English)	, 構造II, , pp. 511-512
発行日 / Pub. date	2024, 8
権利情報	一般社団法人 日本建築学会

Zero-Crossing-Rate Based Global Damping Model of VE Systems Considering Frequency Sensitivity

正会員 ○張庭維*

同 佐藤大樹**

Wind-Induced Response, Global Damping Model, Viscoelastic, Frequency Sensitivity, Zero Crossing Rate.

1. Introduction

To well model the viscoelastic (VE) damper, the fractional derivative (FD) model can express the strain, temperature, and frequency dependency [1]. The wind time [2] (memorizing past data) is required for calculating the FD model, and the amount of data to be stored becomes enormous in the case of a long-period motion such as a wind response. Therefore, it is unsuitable for wind response analysis of high-rise buildings with many VE dampers installed. The global damping (GD) model [3], which is expressed by only two parameters considering the natural frequency and damping ratio, is easily used for the wind-resistance design of the VE-damped structures but lacks considering its frequency dependency. The paper aims to propose a zero-crossing-rate-based method to simplify the frequency-sensitive VE-damped structure into the GD model considering the coupling effect by its frequency dependency and wind.

2. Target building and analytical model

The height of the target building is a $H = 200$ m with an aspect ratio $H/\sqrt{BD} = 4.0$, whose $D = B = 50$ m. Due to the wind-induced response of high-rise buildings is mainly caused by the contribution of the 1st mode [4], the simulation in this study focused on the 1st modal single-degree of freedom (SDOF) model, including the frame with frame damping, the brace, and a VE damper (Fig. (1)). In the simulation, the natural period of frame is set as $T_f = 0.02H$. The 1st modal stiffness K_f and damping coefficient C_f of the frame can be obtained by Eq. (1, 2).

$$K_f = M\left(\frac{2\pi}{T_f}\right)^2 = M\omega_f^2 \quad , \quad C_f = 2M\omega_f\xi_f(\omega_f) \qquad (1, 2)$$

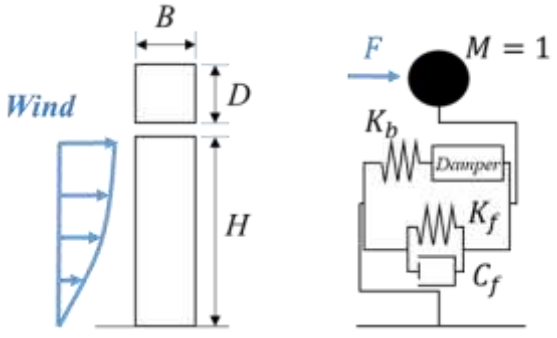

(a) Target building (b)SDOF model

Fig. 1. Target building

3. Analytical wind

Fig. (2) shows examples of the 1st modal analytical wind force in the (a) along-wind and (b) across-wind directions in the time history. For the along-wind force, to avoid the transient response in time-history analysis, the first and last 50 s were modified by envelope. Fig. (3) shows the 10-ensemble-averaging normalized power spectral density (PSD) of the 1st modal analytical wind force, in the along-wind (in red) and across-wind (in blue) directions. The PSD of the along-wind had the high power of a wide band at low frequencies. In contrast, the normalized PSD of the across-wind had a peak close to the frequency of 0.1 Hz.

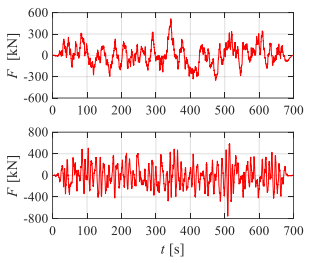

Fig. 2. Time history of wind force (a) along-wind without mean, (b) across-wind

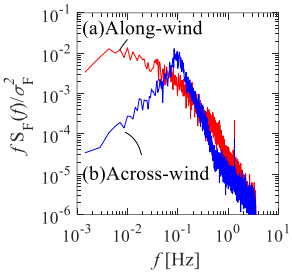

Fig. 3. Normalized PSD of wind force by 10-ensemble-averaging

4. VE systems

4.1. Resonance-frequency-based GD (RF-GD) model

The GD model (Fig. (4)) is commonly used in the wind-resistance design code for the damper.

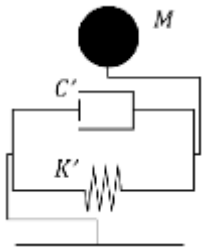

Fig. 4. GD model

To simplify the FD model into the GD model considering resonance frequency, this study names it the resonance-frequency-based global damping (RF-GD) model. The equivalent stiffness K' and damping coefficient C' of the RF-GD model are obtained, which is given by Eq. (3a, b) [1].

$$K' = K_f + K'_a(\omega_n) \qquad (3a)$$

$$C' = 2M\omega_n\left[\frac{C_f}{2M\omega'_n(\omega_n)} + \frac{\eta(\omega_n)}{2}\right] \qquad (3b)$$

4.2. Zero-crossing-rate based GD (ZR-GD) model

The equivalent stiffness K' and damping coefficient C' of the ZR-GD model are defined with the zero crossing rate ω_{ZR}, given by Eq. (4a, b).

$$K' = K_f + K'_a(\omega_{ZR}) \tag{4a}$$

$$C' = 2M\omega_{ZR}\left[\frac{C_f}{2M\omega'_n(\omega_{ZR})} + \frac{\eta(\omega_{ZR})}{2}\right] \tag{4b}$$

The zero crossing rate ω_{ZR} can be obtained by the standard derivations (σ_D, σ_V, σ_A, and σ_J) [1], given by Eq. (5). There are six kinds of ω_{ZR} for wind-induced responses. When considering the along-wind responses, the standard deviation used along-wind responses (including displacement, velocity, and acceleration); when considering the across-wind responses, the standard deviation used across-wind responses, respectively.

$$\omega_{ZR} = \begin{cases} \sigma_{V,AL}/\sigma_{D,AL}, & \text{Disp. in along-wind direction.} \\ \sigma_{A,AL}/\sigma_{V,AL}, & \text{Velo. in along-wind direction.} \\ \sigma_{J,AL}/\sigma_{A,AL}, & \text{Acc. in along-wind direction.} \\ \sigma_{V,AC}/\sigma_{D,AC}, & \text{Disp. in across-wind direction.} \\ \sigma_{A,AC}/\sigma_{V,AC}, & \text{Velo. in across-wind direction.} \\ \sigma_{J,AC}/\sigma_{A,AC}, & \text{Acc. in across-wind direction.} \end{cases} \tag{5}$$

Where σ_D, σ_V, σ_A, and σ_J can be obtained by Eq. (6a-d).

$$\sigma_D = \sqrt{\int_0^\infty |H_D(i\omega)|^2 S_F(i\omega)\, d\omega}, \tag{6a}$$

$$\sigma_V = \sqrt{\int_0^\infty |i\omega H_D(i\omega)|^2 S_F(i\omega)\, d\omega}, \tag{6b}$$

$$\sigma_A = \sqrt{\int_0^\infty |-\omega^2 H_D(i\omega)|^2 S_F(i\omega)\, d\omega}, \tag{6c}$$

$$\sigma_J = \sqrt{\int_0^\infty |-i\omega^3 H_D(i\omega)|^2 S_F(i\omega)\, d\omega}, \tag{6d}$$

Here, $H_D(i\omega)$ is the displacement transfer functions of the system [1]; $S_F(i\omega)$ is the PSD of wind force.

5. Comparison of wind-induced responses

Fig. (5) shows the FD, RF-GD, and ZR-GD models' displacement responses in the along- and across-wind direction, respectively. Fig. (5a-i) and Fig. (5b-i) express that the maximum displacement of the RF-GD of the 2H-HH-00 model (an added component has both the hard stiffness of the brace and damper with no frame damping has a massive difference from that of the FD model; but, the maximum displacement of the ZR-GD of the 2H-HH-00 model matches the FD model well. In contrast, Fig. (5a-ii) and Fig. (5b-ii) express the RF-GD and ZR-GD of the 2H-SS-00 model has the same trend of displacement response as the FD model.

Fig. (6) show the comparison of the accuracy of the maximum of along- and across-wind responses respectively of RF-GD model and ZR-GD model with no frame damping. The ZR-GD models that match the maximum of the FD models well have better agreements than the RF-GD models.

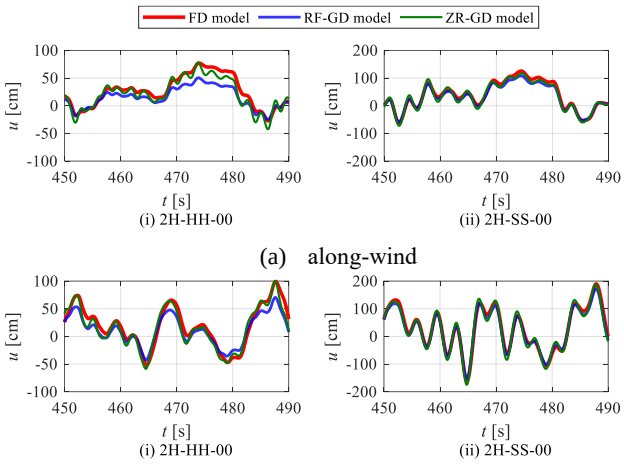

(a) along-wind

(b) across-wind

Fig. 5. Displacement of the FD, RF-GD, and ZR-GD models

6. Conclusions

This paper proposed the ZR-GD models for tall VE-damped buildings subjected to along- and across-wind forces, respectively. The behavior of the ZR-GD model of the VE-damped structure is described by a SDOF model, which considers the characteristics of both the frequency-sensitive fractional derivative model and wind excitation. Compared with the conventional RF-GD model, the ZR-GD model is verified with high accuracy by the fractional derivative model of the VE-damped structure.

References

[1] D. Sato, T.-W. Chang, Prediction on wind-induced responses for tall buildings considering frequency dependency of viscoelastic damped structures, The Structural Design of Tall and Special Buildings (2024) e2094

[2] Sato, D., Chang, T. W., & Chen, Y. (2022). Effects of Different Frequency Sensitivity Models of a Viscoelastic Damper on Wind-Induced Response of High-Rise Buildings. Buildings, 12(12), 2182.

[3] K. Kasai, K. Okuma, Evaluation rule and its accuracy for equivalent period and damping of frequency-dependent passive control systems [in japanese], Journal of Structural and Construction Engineering 580 (2004) 51–59.

[4] Hirai, H.; Yoshie, K.; Sato, D.; Suzuki, Y.; Kitamura, H. Characteristic of higher mode response of high-rise building under fluctuating wind force [in Japanese]. AIJ Journal of Technology and Design 2012, 18, 79–84.

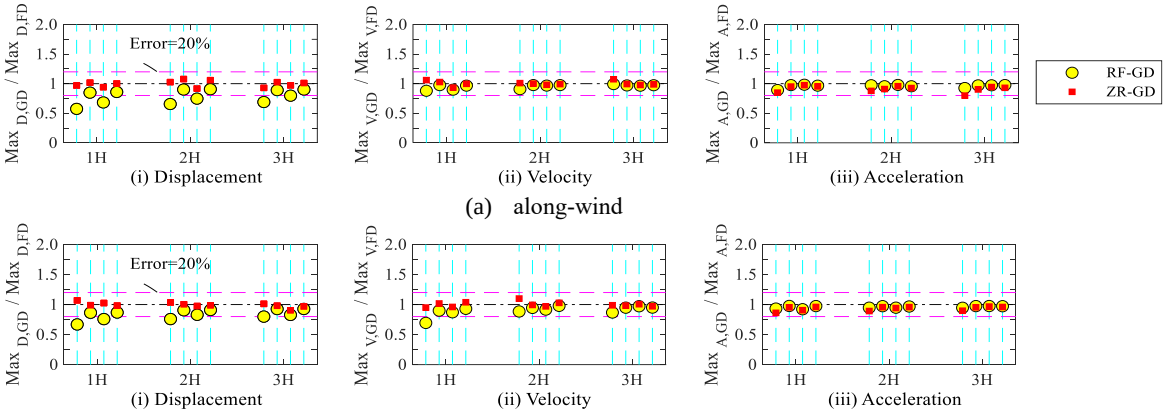

(a) along-wind

(b) across-wind

Fig. 6. Comparison of maximum responses: (HH, SH, HS, SS from left to right of each frame)

*東京工業大学環境・社会理工学院　大学院生

**東京工業大学科学技術創成研究院　准教授・博士（工学）

* Doctoral Student, School of Environment and Society, Tokyo Institute of Technology

** Associate Prof. , IIR, Tokyo Institute of Technology, Dr. Eng.